

Grant-Free Random Access of IoT devices in Massive MIMO with Partial CSI

Gilles Callebaut¹, François Rottenberg¹, Liesbet Van der Perre¹, and Erik G. Larsson²

¹Department of Electrical Engineering (ESAT-DRAMCO), KU Leuven, 9000 Ghent, Belgium

²Department of Electrical Engineering (ISY), Linköping University, Linköping, Sweden

Abstract—The number of wireless devices is drastically increasing, resulting in many devices contending for radio resources. In this work, we present an algorithm to detect active devices for unsourced random access, *i.e.*, the devices are uncoordinated. The devices use a unique, but non-orthogonal preamble, known to the network, prior to sending the payload data. They do not employ any carrier sensing technique and blindly transmit the preamble and data. To detect the active users, we exploit partial channel state information (CSI), which could have been obtained through a previous channel estimate. For static devices, *e.g.*, Internet of Things nodes, it is shown that CSI is less time-variant than assumed in many theoretical works. The presented iterative algorithm uses a maximum likelihood approach to estimate both the activity and a potential phase offset of each known device. The convergence of the proposed algorithm is evaluated. The performance in terms of probability of miss detection and false alarm is assessed for different qualities of partial CSI and different signal-to-noise ratio.

Index Terms—activity detection, grant-free, massive MIMO, maximum likelihood, random access.

I. INTRODUCTION

Massive machine-typed communication (mMTC) is envisioned to enable low-power connectivity to a very large number of devices and open up new applications. While it has been put forward as a key building block in 5G and beyond, it has so far received less attention than enhanced Mobile Broadband (eMBB) and Ultra-Reliable Low Latency Communications (URLLC). The challenge in mMTC, and in general Internet of Things (IoT) systems, resides in the low-power operation, sporadic nature of the traffic and a large amount of uncoordinated devices. As these devices are often battery-powered, they are constrained in the signalling overhead they can handle [2]. Furthermore, they are often deployed in remote areas, where network coverage is low or non-existent [2, 3]. To address this, novel protocols need to be designed tailored to the low-power, sporadic and massive nature of mMTC traffic. One promising direction, and the focus of this work, is the use of massive MIMO, where a large number of antennas is present at the base station.

Two multiple access approaches can be taken, grant-based and grant-free random access. The former requires the devices to obtain a grant from the network, where after it can use a

collision-free radio resource to transmit its data. The disadvantage of this approach for IoT and mMTC is that devices need to compete for grants, requiring, *e.g.*, dedicated preambles or a lot of signalling for collision resolution. Due to the number of competing devices such schemes are not practical and scalable.

Therefore, grant-free approaches are advocated over grant-based solutions [4–6]. In grant-free random access, devices do not contend for a grant, but just access the network when required. Often these devices are unaware of the other devices in the system and operate in an uncoordinated fashion, which is called unsourced grant-free random access [6]. Different approaches have been studied to detect the active devices in massive MIMO systems. Detecting active devices is facilitated when each device uses a unique and orthogonal preamble sequence. This entails that each preamble should have the same length as the number of devices to have no collisions, which is unpractical. Therefore a number of studies have considered a pool of orthogonal pilots [7] or the use of non-orthogonal pilots. Both of these strategies have been elaborated in [4], where they formulate the device-activity detection problem as a compressed sensing problem, where the sparsity of the active devices at each time slot is exploited. However, compressed sensing requires the preamble length to be larger than the active devices, increasing the energy expenditure of data transfer. To combat this, in [6, 8] a covariance-based method is suggested using two estimators for device activity recovery, *i.e.*, maximum-likelihood (ML) and non-negative least squares (NNLS). This work is generalized by Ganesan, Bjornson, and Larsson [9, 10] to the cell-free case where multiple access points (APs) are geographically distributed. They considered different large-scale fading coefficients per APs. They employed a simplification of their proposed algorithm by including only the AP with the strongest contribution. They concluded that co-located massive MIMO is highly sensitive to low signal-to-noise ratios (SNRs), while cell-free deployment is better suited against shadowing fading effects.

Contributions. Inspired by these works, we propose a new algorithm exploiting the static nature of IoT devices. As demonstrated in [11] and elaborated in Section II, the channel state information (CSI) can remain almost invariant over large period of times (hours) for scenarios with low mobility. This was not yet leveraged by practical algorithms in the literature to the best of our knowledge. Given that the base station knows a part of the CSI of each device the performance of the device activity scheme can be improved. To do so, we formulate the maximum-likelihood activity detection problem using partial CSI. Furthermore, a phase offset can be estimated which occurs due to carrier frequency offset (CFO) (when

The research reported herein was partly funded by the European Union’s Horizon 2020 research and innovation programme under grant agreement No 101013425.

This paper is presented at IEEE WCNC 2023. G. Callebaut, F. Rottenberg, L. Van der Perre, and E. G. Larsson, “Grant-Free random access of IoT devices in massive MIMO with partial CSI,” in *2023 IEEE Wireless Communications and Networking Conference (WCNC) (IEEE WCNC 2023)*, Glasgow, United Kingdom (Great Britain), Mar. 2023

the CFO is static over the preamble duration). We validate the convergence of the iterative algorithm, study the impact of different initialization vectors for the device activity, the impact of the quality of the partial CSI and the SNR on the performance of the algorithm.

The used mathematical notations are described in <https://github.com/wavecore-research/math-notations>.

II. MOTIVATION – RECURRENCE IN CSI

IoT technologies are often put in the field with a deploy-and-forget strategy, where the devices remain immobile afterwards. As such, we can expect that the channel conditions are less time-variant than typically assumed in literature [12, 13]. An experimental campaign to investigate the long-term behavior of the channel is presented in [11]. The long-term behavior is measured by taking the channel correlation $\delta_{i,j} = |\bar{\mathbf{h}}_i^H \cdot \bar{\mathbf{h}}_j| / \|\bar{\mathbf{h}}_i\| \|\bar{\mathbf{h}}_j\|$ of the first channel estimate and the other channel N measurements, i.e., $\delta_{1,j}$ for $j \in \{1, \dots, N\}$.

The observed channel correlations are depicted in Fig. 1. It illustrates that most of the time the correlation coefficient is close to 1, indicating that the channel is highly correlated with the first estimate and thus can be considered static. It also shows that, while in some occasions the correlation drops, the channel quickly becomes again highly correlated with the first channel instance. More than 90% of the measured channels¹ have a correlation coefficient higher than 0.9. This demonstrates the potential of re-using channel estimates in IoT contexts.²

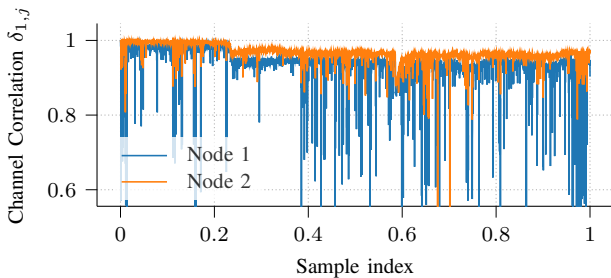


Figure 1: Channel correlation over a full day (9h24-17h48) with over 10 000 channel instances, with an average correlation of 0.935/0.968 and a standard deviation of 0.06/0.03 for Node 1/Node 2.

III. SYSTEM MODEL

There is a total of K single-antenna devices and a total of M co-located base station (BS) antennas. The set of active users trying to access the network is denoted by \mathcal{K}_a , with $|\mathcal{K}_a| \leq K$. To access the network, each active device $k \in \mathcal{K}_a$ sends a unique, non-orthogonal preamble of length T , known to the network. The pilot symbol of the preamble sent by device k at pilot symbol t is denoted by $s_{k,t}$. The channel vector between the receive antenna m and user k is denoted by $h_{k,m} \in \mathbb{C}$, and

¹More specifically, 91% and 95% for Node 1 and Node 2, respectively.

²We use here the term “re-using” to indicate that we no longer operate in a block fading model with independent channel realizations. Typically, these blocks are considered in the order of 50 ms.

is considered fixed over the preamble duration. The received symbol at the m -th BS antenna at time t is

$$y_{t,m} = \sum_{k=0}^{K-1} h_{k,m} s_{k,t} \gamma_k + w_{t,m}, \quad (1)$$

where γ_k is an unknown complex scalar and $w_{t,m} \in \mathbb{C}$ is independently and identically distributed (i.i.d.) zero mean circularly symmetric complex Gaussian (ZMCSCG) noise with variance σ^2 . The unknown complex scalar γ_k can be developed as

$$\gamma_k = \sqrt{\rho_k} a_k e^{j\phi_k}, \quad (2)$$

where $\rho_k \in \mathbb{R}^+$ is the transmit power of device k , $a_k \in \{0, 1\}$ is the device activity and ϕ_k models a potential phase offset. This offset ϕ_k can account for a CFO, where the phase is considered constant over the preamble duration. This occurs when no frequency drift has occurred during the preamble duration, which is a feasible assumption as the CFO is typically low, yielding negligible phase rotations during the preamble interval. By assuming that all M antennas are perfectly synchronized, this offset is only dependent on the device. In case the device is inactive, γ_k will be zero. We will introduce the term *activity indicator* to denote γ_k .

Let us consider that the BS knows a part of the CSI, i.e., $g_{k,m}$ in

$$h_{k,m} = g_{k,m} + \lambda_k \epsilon_{k,m}, \quad (3)$$

where $\epsilon_{k,m}$ are i.i.d. ZMCSCG variables with unit variance, and $\lambda_k \in \mathbb{R}^+$ models the unknown part of the CSI. The large-scale fading coefficient of user k is $\beta_k = \mathbb{E}(\|\mathbf{h}_k\|^2 / M) = \|\mathbf{g}_k\|^2 / M + \lambda_k^2$. The factor λ_k models the quality of the known CSI. Hence, it quantifies the correlation of the actual channel $h_{k,m}$ to the known partial CSI $g_{k,m}$. In the extreme case with $\lambda_k = 0$, the CSI is perfectly known and there is no uncertainty left, as was studied in [11]. This could be the case in a fully static environment and if the CSI estimates are noiseless. However, for a realistic IoT scenario, even for static devices, CSI is not perfect due to i) environment dynamics and ii) noisy estimates. The parameter λ_k then quantifies this imperfection. It is here assumed to be known³. Another extreme case, as considered in [8, 10], is obtained when $g_{k,m} = 0, \forall m$, implying that only the large scale fading coefficient of user k is known, i.e., $\lambda_k = \sqrt{\beta_k}$.

IV. DEVICE ACTIVITY DETECTION

This section describes the proposed activity detection algorithm. First, the log-likelihood of the received preamble is derived. Then, given its non-convex expression, an iterative approach is proposed to estimate the parameters $\gamma_k \forall k$. Finally, activity detection is performed.

A. Log-Likelihood of the Received Symbols

Combining (1) and (3), the symbol, received at BS antenna m and for pilot symbol t , is given by

$$y_{t,m} = \sum_{k=0}^{K-1} (g_{k,m} + \epsilon_{k,m} \lambda_k) s_{t,k} \gamma_k + w_{t,m}.$$

³It could be set to a certain value depending on the user activity profile and/or tracked for each user over time.

Stacking the observations at antenna m gives

$$\mathbf{y}_m = \sum_{k=0}^{K-1} g_{k,m} \mathbf{s}_k \gamma_k + \sum_{k=0}^{K-1} \epsilon_{k,m} \lambda_k \mathbf{s}_k \gamma_k + \mathbf{w}_m,$$

where

$$\mathbf{y}_m = \begin{pmatrix} y_{0,m} \\ \vdots \\ y_{T-1,m} \end{pmatrix}, \quad \mathbf{s}_k = \begin{pmatrix} s_{0,k} \\ \vdots \\ s_{T-1,k} \end{pmatrix}, \quad \mathbf{w}_m = \begin{pmatrix} w_{m,0} \\ \vdots \\ w_{m,T-1} \end{pmatrix}.$$

For a given value of γ_k , $\mathbf{y}_m | \gamma_k$ has a circularly symmetric Gaussian distribution with mean $\sum_{k=0}^{K-1} g_{k,m} \mathbf{s}_k \gamma_k$. After defining the vector $\boldsymbol{\theta}_m = \sum_{k=0}^{K-1} \epsilon_{k,m} \lambda_k \mathbf{s}_k \gamma_k + \mathbf{w}_m$, the covariance matrix is

$$\mathbf{C} = \mathbb{E}(\boldsymbol{\theta}_m \boldsymbol{\theta}_m^H) = \sum_{k=0}^{K-1} \lambda_k^2 |\gamma_k|^2 \mathbf{s}_k \mathbf{s}_k^H + \sigma^2 \mathbf{I}_T, \quad (4)$$

where we used the fact that $\epsilon_{k,m}$ were assumed to be i.i.d. and the additive noise is white. Note that this covariance matrix does not depend on the antenna index m and is thus valid for all \mathbf{y}_m . Defining the vector $\boldsymbol{\gamma} = (\gamma_0, \dots, \gamma_{K-1})^T$, and $\boldsymbol{\Theta}_m = \mathbf{y}_m - \sum_{k=0}^{K-1} g_{k,m} \mathbf{s}_k \gamma_k$ the log-likelihood of the observation vector \mathbf{y}_m is

$$\log p(\mathbf{y}_m | \boldsymbol{\gamma}) = -\ln(|\mathbf{C}|) - T \ln(\pi) - \boldsymbol{\Theta}_m^H \mathbf{C}^{-1} \boldsymbol{\Theta}_m.$$

Given the conditional independence of $\epsilon_{k,m}$ and $w_{t,m}$ over the antennas, the different \mathbf{y}_m are independent as well. Hence, the log-likelihood of the aggregated observations at all antennas $\mathbf{y} = (\mathbf{y}_0^T, \dots, \mathbf{y}_{M-1}^T)^T$ becomes

$$\log p(\mathbf{y} | \boldsymbol{\gamma}) = -M \ln(|\mathbf{C}|) - MT \ln(\pi) - \sum_{m=0}^{M-1} \boldsymbol{\Theta}_m^H \mathbf{C}^{-1} \boldsymbol{\Theta}_m. \quad (5)$$

B. Iterative Algorithm for Maximizing Likelihood

The maximum likelihood estimator of $\boldsymbol{\gamma}$ is obtained by maximizing

$$\hat{\boldsymbol{\gamma}}_{\text{ML}} = \arg \max_{\boldsymbol{\gamma}} \log p(\mathbf{y} | \boldsymbol{\gamma}).$$

This problem is not trivial to solve given the nonlinear and non-convex dependence of the log-likelihood, more specifically the covariance matrix \mathbf{C} , in $\boldsymbol{\gamma}$. An idea to maximize the likelihood is to use an iterative approach, similarly as [8, 10]: at each iteration, all γ_k are kept fixed but one, which is optimized and updated. This way, they get updated one by one until convergence is attained, *i.e.*, a maximum number of iterations or a certain tolerance is reached. A block diagram of the algorithm is given in Figure 2 and the pseudocode is summarized in Algorithm 1.

Let us consider that the complex-valued $\gamma_{k'}$ needs to be updated. Using the definition introduced in (2), we can rewrite $\gamma_{k'}$ with a phase-amplitude decomposition: $\gamma_{k'} = r_{k'} e^{j\phi_{k'}}$, with $r_{k'} = |\gamma_{k'}| = \sqrt{\rho_{k'}} a_{k'}$. The optimization with respect to $\gamma_{k'}$ is done in the following in several steps: i) optimizing the phase $\phi_{k'}$ for a fixed value of $r_{k'}$, ii) re-inserting this expression in the objective function to remove the dependence in $\phi_{k'}$ and iii) optimizing the amplitude $r_{k'}$.

1) *Phase optimization:* To highlight the dependence of the objective function in $\gamma_{k'}$ for constant values of other γ_k , $k \neq k'$, let us define the vector

$$\mathbf{y}_{k',m} = \mathbf{y}_m - \sum_{k=0, k \neq k'}^{K-1} g_{k,m} \mathbf{s}_k \gamma_k, \quad (8)$$

which can be seen as a cancellation of device interference to isolate the contribution from device k' . Hence, the objective function to maximize can be written as in (7)⁴.

where we explicitly express the dependence in $(r_{k'}, \phi_{k'})$ while the other $(r_k, \phi_k), k \neq k'$ do not appear since they are considered constant. Note that the matrix \mathbf{C} , defined in (4), does not depend on $\phi_{k'}$ but only $r_{k'}$. In the extreme case of no prior CSI, *i.e.*, $g_{k',m} = 0 \forall m$, the dependence of $f(r_{k'}, \phi_{k'})$ in $\phi_{k'}$ disappears and there is an underdetermination and no estimate of the phase offset can be obtained. In other cases, we can find that, after some manipulations,

$$\hat{\phi}_{k'} = \angle \mathbf{s}_{k'}^H \mathbf{C}^{-1} \sum_{m=0}^{M-1} g_{k',m}^* \mathbf{y}_{k',m}. \quad (9)$$

This result has an intuitive understanding: the optimal phase $\phi_{k'}$ tends to align the partial CSI with the observations due to device k' .

2) *Removing the phase dependence:* Inserting this optimal value in the objective function $f(r_{k'}, \phi_{k'})$ makes the dependence in $\phi_{k'}$ vanish and gives (6).

3) *Amplitude optimization:* To alleviate the dependence on $r_{k'}$ in (6), let us define

$$\begin{aligned} \mathbf{C}_{-k'} &= \mathbf{C} - \lambda_{k'}^2 |\gamma_{k'}|^2 \mathbf{s}_{k'} \mathbf{s}_{k'}^H \\ &= \sum_{k \in k'} \lambda_k^2 |\gamma_k|^2 \mathbf{s}_k \mathbf{s}_k^H + \sigma^2 \mathbf{I}_T, \end{aligned} \quad (10)$$

which does not depend on $r_{k'}$ and is full rank, thus invertible. Applying the Sherman-Morrison formulas [14] to \mathbf{C}^{-1} and $\mathbf{C}_{-k'}^{-1} \mathbf{s}_{k'}$ gives

$$\mathbf{C}^{-1} = \mathbf{C}_{-k'}^{-1} - \frac{\mathbf{C}_{-k'}^{-1} \mathbf{s}_{k'} \mathbf{s}_{k'}^H \mathbf{C}_{-k'}^{-1} r_{k'}^2 \lambda_{k'}^2}{1 + \mathbf{s}_{k'}^H \mathbf{C}_{-k'}^{-1} \mathbf{s}_{k'} r_{k'}^2 \lambda_{k'}^2} \quad (11)$$

We insert these expressions in (6) and we omit terms that do not depend on $r_{k'}$, which will vanish after taking the derivative. This gives

$$\tilde{f}(r_{k'}) = -M \ln(|\mathbf{C}|) + \frac{\alpha r_{k'}^2 + \beta r_{k'}}{1 + \delta r_{k'}^2}, \quad (12)$$

where we defined the constants (independent of $r_{k'}$) α , β and δ , as

$$\begin{aligned} \alpha &= \sum_{m=0}^{M-1} |\mathbf{y}_{k',m}^H \mathbf{C}_{-k'}^{-1} \mathbf{s}_{k'}|^2 \lambda_{k'}^2 - \mathbf{s}_{k'}^H \mathbf{C}_{-k'}^{-1} \mathbf{s}_{k'} \sum_{m=0}^{M-1} |g_{k',m}|^2 \\ \beta &= 2 \left| \sum_{m=0}^{M-1} \mathbf{y}_{k',m}^H \mathbf{C}_{-k'}^{-1} \mathbf{s}_{k'} g_{k',m} \right| \\ \delta &= \mathbf{s}_{k'}^H \mathbf{C}_{-k'}^{-1} \mathbf{s}_{k'} \lambda_{k'}^2. \end{aligned} \quad (13)$$

⁴For clarity, we omit in the following the constant term $MT \ln(\pi)$ which does not affect optimization as it does not depend on $\boldsymbol{\gamma}$ and vanishes after differentiation.

$$f(r_{k'}) = -M \ln(|\mathbf{C}|) - \sum_{m=0}^{M-1} \mathbf{y}_{k',m}^H \mathbf{C}^{-1} \mathbf{y}_{k',m} - r_{k'}^2 \mathbf{s}_{k'}^H \mathbf{C}^{-1} \mathbf{s}_{k'} \sum_{m=0}^{M-1} |g_{k',m}|^2 + 2 \left| \sum_{m=0}^{M-1} \mathbf{y}_{k',m}^H \mathbf{C}^{-1} \mathbf{s}_{k'} g_{k',m} \right| r_{k'} \quad (6)$$

$$f(r_{k'}, \phi_{k'}) = -M \ln(|\mathbf{C}|) - \sum_{m=0}^{M-1} (\mathbf{y}_{k',m} - g_{k',m} \mathbf{s}_{k'} r_{k'} e^{j\phi_{k'}})^H \mathbf{C}^{-1} (\mathbf{y}_{k',m} - g_{k',m} \mathbf{s}_{k'} r_{k'} e^{j\phi_{k'}}) \quad (7)$$

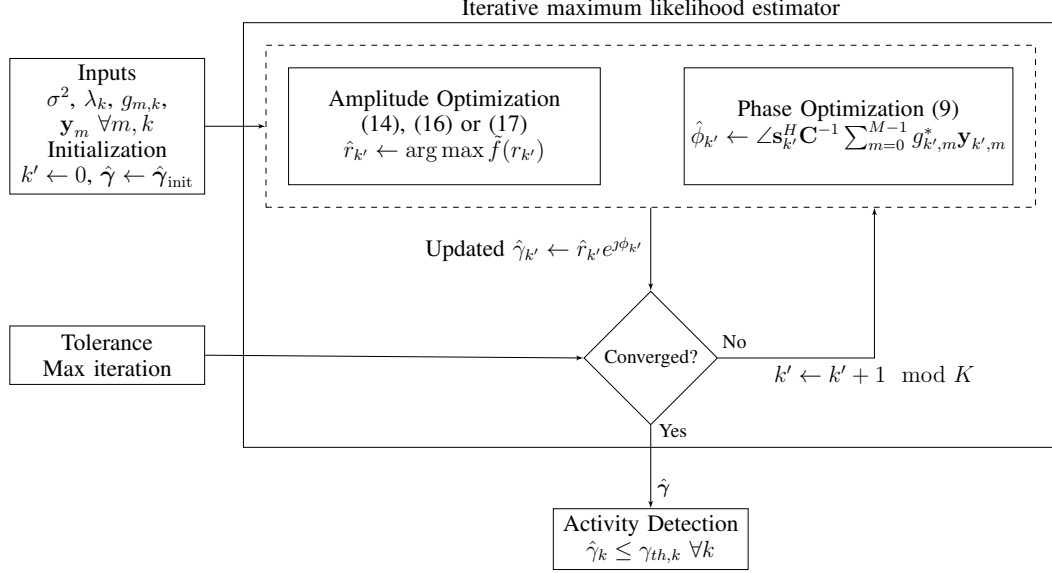


Figure 2: Block diagram of the iterative maximum likelihood estimator and activity detection.

One can note that $\tilde{f}(r_{k'})$ in (12) can now be differentiated with respect to $r_{k'}$, using the differential rule $\partial(\log |\mathbf{A}|) = \text{tr}[\mathbf{A}^{-1} \partial \mathbf{A}]$. Setting the derivative to zero gives, noting that the denominator is always strictly positive,

$$0 = -r_{k'}^3 2M\delta^2 - r_{k'}^2 \beta \delta + r_{k'} (-2M\delta + 2\alpha) + \beta, \quad (14)$$

which is a polynomial of degree 3 in $r_{k'}$. There are closed-form solutions for the roots of such polynomials. Following *Descartes's rule of signs*, (14) has only one real and positive root, as required, in case the terms are non-zero. Below we discuss the special cases when the terms are not non-zero, i.e., when there is no or complete CSI knowledge.

The algorithm is summarized in the pseudocode **Algorithm 1**. At each iteration, the constants α , β and δ can be easily re-evaluated based on (13). They require the matrix inversion $\mathbf{C}_{-k'}^{-1}$. To avoid re-computing a full inverse at each iteration, one can rely on the Sherman-Morrison formula and on the current knowledge of \mathbf{C}^{-1} , which is updated at the end of each iteration by inserting the obtained value of $r_{k'}$ in (11). Using (10), we find

$$\mathbf{C}_{-k'}^{-1} = \mathbf{C}^{-1} + \frac{\lambda_{k'}^2 |\gamma_{k'}|^2 \mathbf{C}^{-1} \mathbf{s}_{k'} \mathbf{s}_{k'}^H \mathbf{C}^{-1}}{1 - \lambda_{k'}^2 |\gamma_{k'}|^2 \mathbf{s}_{k'}^H \mathbf{C}^{-1} \mathbf{s}_{k'}}. \quad (15)$$

Moreover, computations can be optimized as several quantities appear multiple times and can be computed only once. The

complexity of the proposed algorithm is $\mathcal{O}(IMT^2)$, where I is the number of iterations.⁵

We now investigate two particular cases, to gain further insights.

Algorithm 1 Iterative maximum likelihood device activity detector

Require: $\sigma^2, \lambda_k, \mathbf{y}_m, g_{k,m}, \hat{\gamma}_{\text{init}} \forall k, m$
 $k' \leftarrow 0$
 $\hat{\gamma} \leftarrow \hat{\gamma}_{\text{init}}$
 $\mathbf{C}^{-1} \leftarrow \left(\sum_{k=0}^{K-1} \lambda_k^2 |\hat{\gamma}_k|^2 \mathbf{s}_k \mathbf{s}_k^H + \sigma^2 \mathbf{I}_T \right)^{-1}$
while Not converged **do**
 Compute $\mathbf{y}_{k',m}, \mathbf{C}_{-k'}^{-1}, \alpha, \beta$ and δ based on (8), (15) and (13)
 $\hat{r}_{k'} \leftarrow \arg \max \tilde{f}(r_{k'})$ ▷ Update amplitude based on (14), (16) or (17)
 $\hat{\phi}_{k'} \leftarrow \angle \mathbf{s}_{k'}^H \mathbf{C}^{-1} \sum_{m=0}^{M-1} g_{k',m}^* \mathbf{y}_{k',m}$ ▷ Update phase
 $\hat{\gamma}_{k'} \leftarrow \hat{r}_{k'} e^{j\hat{\phi}_{k'}}$
 $\mathbf{C}^{-1} \leftarrow \mathbf{C}_{-k'}^{-1} - \frac{\mathbf{C}_{-k'}^{-1} \mathbf{s}_{k'} \mathbf{s}_{k'}^H \mathbf{C}_{-k'}^{-1} r_{k'}^2 \lambda_{k'}^2}{1 + \mathbf{s}_{k'}^H \mathbf{C}_{-k'}^{-1} \mathbf{s}_{k'} r_{k'}^2 \lambda_{k'}^2}$
 $k' \leftarrow k' + 1 \pmod K$
end while

a) *Particular case: device with no CSI:* Now consider that, for a given k' , $g_{k',m} = 0 \forall m$. This could be because this device is new or moving a lot, such that its CSI is outdated. Only, its parameter $\lambda_{k'}$ is known, which is equal

⁵Note that I will in practice depend on K as we will iterate N times over all users K , but this is not a requirement.

to the large-scale fading coefficient $\sqrt{\beta_{k'}}$. At iteration of user k' , evaluating (13) for $g_{k',m} = 0 \forall m$ implies that $\beta = 0$. Hence, (14) simplifies to

$$0 = 2r_{k'}(-r_{k'}^2 M \delta^2 - M \delta + \alpha),$$

which has a trivial solution in $r_{k'} = 0$. One of the other roots is always negative. Keeping only the positive one, we find the amplitude update

$$\hat{r}_{k'} = \sqrt{\frac{\alpha - M \delta}{M \delta^2}}. \quad (16)$$

If this root is imaginary, we set $\hat{r}_{k'}$ to zero. As discussed before introducing the phase update equation (9), in the case of no prior CSI, the phase ambiguity cannot be resolved. This particular case gives an update relatively similar to the maximum likelihood estimator derived in [8, (23)], where their ML expression estimates the error, while ours estimates directly the coefficient $\hat{r}_{k'}$, given the same estimate of $\gamma_{k'}$ at each iteration.

b) Particular case: device with complete prior CSI: Now, consider that, for a given k' , $\lambda_{k'} = 0$, so that the CSI is perfectly known. Only the phase shift and the transmit power are unknown. At iteration of user k' , evaluating (13) for $\lambda_{k'} = 0$ implies that $\delta = 0$. Hence, (14) simplifies to a linear equation $0 = r_{k'} 2\alpha + \beta$, which gives the following amplitude update

$$\hat{r}_{k'} = \frac{-\beta}{2\alpha} = \frac{|\mathbf{s}_{k'}^H \mathbf{C}^{-1} \sum_{m=0}^{M-1} g_{k',m}^* \mathbf{y}_{k',m}|}{\mathbf{s}_{k'}^H \mathbf{C}^{-1} \mathbf{s}_{k'} \sum_{m'} |g_{k',m'}|^2}, \quad (17)$$

while the phase is updated according to (9).

4) Initialization: To start the iterative algorithm, we consider different choices to initialize $\hat{\gamma}_{\text{init}}$. A simple choice is to initialize to zero, *i.e.*, $\hat{\gamma}_{\text{init}}^0 = \mathbf{0}$. Another choice is to initialize solely based on the available prior CSI, considering that $\lambda_k \approx 0, \forall k$. The estimator is similar to [11], except that, here, prior CSI is used instead of complete CSI.

If $\lambda_k \approx 0, \forall k$, the covariance matrix \mathbf{C} , defined in (4), simplifies to $\mathbf{C} = \sigma^{-2} \mathbf{I}_T$, which is independent of γ_k . Hence, many terms of the log-likelihood in (5) become independent of γ . Maximizing (5) becomes equivalent to the following minimization

$$\begin{aligned} \max_{\gamma} \log p(\mathbf{y}|\gamma) &= \min_{\gamma} \sum_{m=0}^{M-1} \left\| \mathbf{y}_m - \sum_{k=0}^{K-1} g_{k,m} \mathbf{s}_k \gamma_k \right\|^2 \\ &= \min_{\gamma} \|\mathbf{y} - \mathbf{\Gamma} \gamma\|^2, \end{aligned}$$

where we defined the vector and matrix notations

$$\begin{aligned} \mathbf{y} &= (\mathbf{y}_0 \dots \mathbf{y}_{M-1})^T, \quad \mathbf{\Gamma} = (\mathbf{\Gamma}_0 \dots \mathbf{\Gamma}_{M-1})^T, \\ \mathbf{\Gamma}_m &= (\mathbf{s}_0 \dots \mathbf{s}_{K-1}) \text{diag}(g_{0,m} \dots g_{K-1,m}). \end{aligned}$$

This minimization problem is a quadratic function of γ , which is a least squares problem. The estimate has the following closed-form expression

$$\hat{\gamma}_{\text{init}}^{\text{ZF}} = \left(\mathbf{\Gamma}^H \mathbf{\Gamma} \right)^{-1} \mathbf{\Gamma}^H \mathbf{y}. \quad (18)$$

This last estimator can be seen as a zero-forcing (ZF) estimator, which requires a matrix inversion. To avoid ill-conditioning, a first necessary condition is that $K \leq MT$.

This condition is not sufficient as the channel and preamble of two devices could be correlated, especially when K is on the order of MT . Moreover, if no prior information is available for a given user k' , *i.e.*, $g_{k',m} = 0, \forall m$, the inverse will also be ill-conditioned. This implies that the k' -th column of $\mathbf{\Gamma}$ becomes null and thus $\mathbf{\Gamma}$ is rank deficient. Moreover, the prior CSI might be noisy, leading to unstable results.

To make initialization more robust, we can use an least minimum mean square error (LMMSE) criterion. To do this, some prior knowledge must be assumed on the statistics of γ , more specifically, its first and second order moments. We here make the following assumptions: i) the activity of each device is independent of one another, ii) the average activity and average transmit power of each device is known and iii) no prior information is known on the phase offset so that ϕ_k is considered uniformly distributed between 0 and 2π . Under these assumptions, we have $\mathbb{E}(\gamma) = \mathbf{0}$ and $\mathbf{D} = \mathbb{E}(\gamma \gamma^H) = \text{diag}(\mathbb{E}(a_0) \mathbb{E}(\rho_0), \dots, \mathbb{E}(a_{K-1}) \mathbb{E}(\rho_{K-1}))$. Hence, for the linear observation model $\mathbf{y} = \mathbf{\Gamma} \gamma + \mathbf{w}$, still considering that $\lambda_k \approx 0, \forall k$, the LMMSE estimator of γ is then given by [15]

$$\hat{\gamma}_{\text{init}}^{\text{LMMSE}} = \left(\mathbf{\Gamma}^H \mathbf{\Gamma} + \sigma^2 \mathbf{D}^{-1} \right)^{-1} \mathbf{\Gamma}^H \mathbf{y}. \quad (19)$$

Note that the matrix to be inverted is always well-conditioned. Finally, a matched filter (MF) estimator could be used to avoid the need for matrix inversion.

$$\hat{\gamma}_{\text{init}}^{\text{MF}} = \left(\text{diag}(\mathbf{\Gamma}^H \mathbf{\Gamma}) + \sigma^2 \mathbf{D}^{-1} \right)^{-1} \mathbf{\Gamma}^H \mathbf{y}. \quad (20)$$

C. Activity Detection

A non-negative activity threshold $\gamma_{\text{th},k}$ is applied for each device k . A device is considered active if $|\hat{\gamma}_k| \geq \gamma_{\text{th},k}$. The real-valued threshold is defined as,

$$\gamma_{\text{th},k} = v \sqrt{\text{SNR}_k}^{-1}, \quad (21)$$

where v is chosen to have a desired probability of false alarm and miss detection performance and with $\text{SNR}_k = M \beta_k / \sigma^2 = \mathbb{E}(\|\mathbf{h}_k\|^2) / \sigma^2 = (\|\mathbf{g}_k\|^2 + M \lambda_k^2) / \sigma^2$.

Miss detection happens when a device was undetected, while it was actually transmitting. Equivalently, a false alarm occurs if a device is considered active by the algorithm but was not. We define the probability of miss detection as the average ratio of undetected devices to the number of active devices $P_{\text{md}} = 1 - \left(|\mathcal{K}_a \cap \hat{\mathcal{K}}_a| / |\mathcal{K}_a| \right)$, where \mathcal{K}_a is the set of active devices and $\hat{\mathcal{K}}_a = \{k | \hat{a}_k = 1, \forall k \in [1, K]\}$ denotes the estimated set of active devices. Note that on average $|\mathcal{K}_a| = K_a$. Similarly, the probability of false alarm is the ratio of inactive devices considered active to the number of inactive devices and is given by $P_{\text{fa}} = \left(|\hat{\mathcal{K}}_a \setminus \mathcal{K}_a| / (K - |\mathcal{K}_a|) \right)$.

A trade-off can be made between the two probabilities by varying v in (21). A lower v yields a lower activity threshold, resulting in more devices considered active. This in turn lowers the probability of miss detection, while increasing the probability of generating a false alarm. In the simulations, the parameter v is swept across the range $[-40, 40]$ dB.

Table I: Simulation parameter set with default values.

Parameter	Symbol	Default value
Number of devices	K	500
Number of total BS antennas	M	64
Signal-to-noise ratio	SNR	20 dB
Device activity probability	ϵ_a	0.1
Pilot sequence	s_k	$\sim \mathcal{CN}(0, 1)$
Pilot length	τ_p	10 symbols
Phase offset	ϕ_k	$\sim \mathcal{U}_{[0, 2\pi]}$
Number of simulations	N_{sim}	>10 000
Number of algorithm iterations	N_{iter}	$K \cdot 4$
Initialization vector	$\hat{\gamma}_{\text{init}}$	$\hat{\gamma}_{\text{init}}^{\text{LMMSE}} (19)$
Unknown part of the CSI	λ	0.3

V. NUMERICAL ASSESSMENT

The default simulation configurations are summarized in Table I. The device activity profile is generated randomly and independently for each device with a probability $\epsilon_a = 0.1$, meaning that on average $\epsilon_a K = 50$ devices are active simultaneously. Or equivalently, the devices have an average duty cycle of 10%, which is high for typical IoT applications [2]. The channel between the BS and device k is modelled as in (3). The pilot sequence is randomly generated from a complex Gaussian distribution $s_k \sim \mathcal{CN}(0, 1)$, and is assumed to be known by the BS. Each device uses a pilot sequence of 10 symbols. A random phase offset $\phi_k \sim \mathcal{U}_{[0, 2\pi]}$ is generated to simulate a carrier frequency offset (considered time-invariant over the preamble duration). The source code for all simulations can be accessed online⁶.

A. Convergence of different initialization vectors

The convergence of different initializations is evaluated with respect to the genie-aided approach. In the genie-aided case, the algorithm is initialized with the real activity indicators, i.e., γ . The convergence is assessed via the likelihood (5) and the mean square error (MSE). The former should monotonically increase with each iteration, while the MSE can vary as it can not directly be minimized. The performance of the different initialization vectors for $\hat{\gamma}_{\text{init}}$ are depicted in Figure 3. The bottom figures zoom in on a smaller region to distinguish the performance of the initialization vectors when converging closer to the genie-aided case. While all initialization methods approximate the genie-aided case, the initialization vector has a non-negligible impact on the performance of the algorithm. An intuitive approach is to initialize with $\mathbf{0}$ because the activity probability is low and hence, on average, 90% of the devices are expected to be inactive. As illustrated in Figure 3, $\hat{\gamma}_{\text{init}} = \mathbf{0}$ requires considerably more iterations to approach the other initialization methods.

B. Impact of the quality of prior CSI

Figure 4 illustrates the performance of the detector algorithms for different correlations between the actual channel and the known CSI, i.e., λ . With increased λ , and thus decreased channel knowledge, both the LMMSE estimator and the proposed algorithm have an increased probability of miss detection. The figure also demonstrates the gain of the

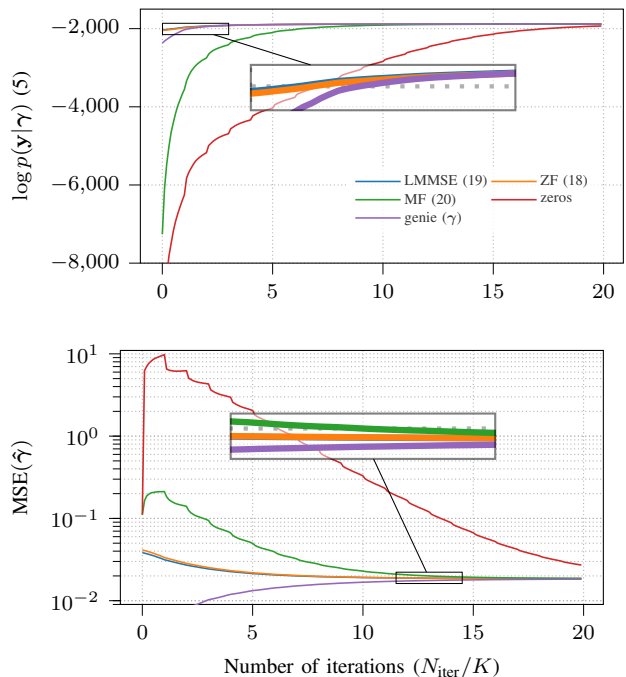


Figure 3: The log-likelihood (5) and MSE of the estimated activity indicators for different initialization vectors. While with all initialization vectors the genie-aided case is approximated, different number of iterations are required.

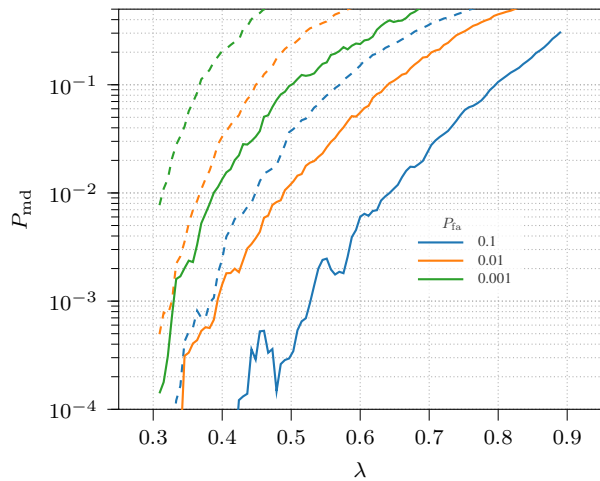


Figure 4: Performance of the proposed algorithm (—) versus the LMMSE estimator (---) for different values of channel knowledge. The probability of miss detection is shown for different values of P_{fa} (10%, 1%, 0.1%).

proposed algorithm with respect to the LMMSE estimator. The algorithm outperforms the LMMSE estimator for all λ and is most effective when the prior CSI has a strong correlation with the actual channel, and diminishes with decreased channel knowledge.

C. Impact of the signal-to-noise ratio

Figure 5 shows the false alarm and miss detection probability of the LMMSE estimator and the iterative maximum likelihood device activity detector for different device SNRs. The full CSI case is included as a baseline for comparison,

⁶<https://github.com/wavecore-research/grant-free-random-access-partial-csi>

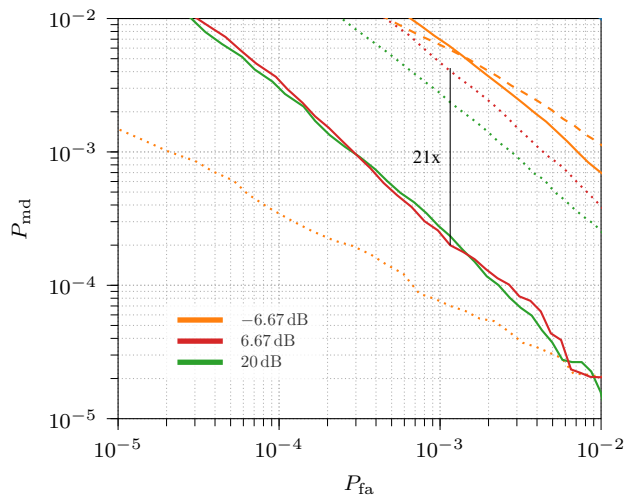


Figure 5: The probability of false alarm and miss detection for different device SNRs for the LMMSE estimator when having full CSI (·····) and partial CSI (---), and the proposed iterative algorithm with partial CSI (—). No miss detection or false alarm occurred in the full CSI case for SNR values of -6.67 dB and 20 dB.

where the full CSI is known instead of only a portion (λ). Fig. 5 demonstrates the large performance gain of the proposed algorithm with respect to the LMMSE estimator. The graph demonstrates that the iterative algorithm lowers the probability of miss detection by a factor of 21 for the same probability of false alarm.⁷ The performance is only marginally increased for very low SNRs (below zero).

VI. CONCLUSION

We formulated an iterative maximum-likelihood (ML) algorithm to detect active devices using prior channel state information (CSI) when performing grant-free random access. Previous experimental work has demonstrated that, in many massive machine-typed communication (mMTC) applications, the CSI is less time-variant than assumed in theoretical models. Given the static nature of Internet of Things (IoT) devices, we have exploited this feature in the activity detection estimator. During grant-free access, the devices transmit a unique, but non-orthogonal preamble, which is used for activity detection. Next to this, the algorithm is also able to detect a device-specific phase offset, which could be caused by carrier frequency offset (CFO). The algorithm is numerically evaluated and compared to the conventional least minimum mean square error (LMMSE) estimator with full channel knowledge and partial CSI. The presented results indicate that the iterative algorithm converges and outperforms the conventional LMMSE estimator. For a signal-to-noise ratio (SNR) of 6.67 dB, the probability of not detecting an active device is 21 times lower for the proposed iterative ML estimator than the LMMSE estimator for the same probability of wrongly considering an inactive device as an active device.

This work can be extended to the cell-free or distributed case with geographically distributed access points. In that case, the partial CSI becomes access point-dependent.

⁷Notably, the LMMSE estimator does not employ an iterative approach. Therefore, our proposed algorithm will be compared in future work with other iterative approaches.

REFERENCES

- [1] G. Callebaut, F. Rottenberg, L. Van der Perre, and E. G. Larsson, "Grant-Free random access of IoT devices in massive MIMO with partial CSI," in *2023 IEEE Wireless Communications and Networking Conference (WCNC) (IEEE WCNC 2023)*, Glasgow, United Kingdom (Great Britain), Mar. 2023.
- [2] G. Callebaut, G. Leenders, J. Van Mulders, G. Ottoy, L. De Strycker, and L. Van der Perre, "The Art of Designing Remote IoT Devices—Technologies and Strategies for a Long Battery Life," *Sensors*, vol. 21, no. 3, 2021, ISSN: 1424-8220. DOI: 10.3390/s21030913. [Online]. Available: <https://www.mdpi.com/1424-8220/21/3/913>.
- [3] S. Wielandt and B. Dafflon, "A local lora based network protocol with low power redundant base stations enabling remote environmental monitoring," in *2020 54th Asilomar Conference on Signals, Systems, and Computers*, 2020, pp. 520–523. DOI: 10.1109/IEEECONF51394.2020.9443344.
- [4] L. Liu, E. G. Larsson, W. Yu, P. Popovski, C. Stefanovic, and E. de Carvalho, "Sparse signal processing for grant-free massive connectivity: A future paradigm for random access protocols in the internet of things," *IEEE Signal Process Mag.*, vol. 35, no. 5, pp. 88–99, Sep. 2018, ISSN: 1053-5888, 1558-0792. DOI: 10.1109/msp.2018.2844952. [Online]. Available: <https://doi.org/10.1109/msp.2018.2844952>.
- [5] J. Ding, D. Qu, H. Jiang, and T. Jiang, "Success probability of grant-free random access with massive MIMO," *IEEE Internet of Things Journal*, vol. 6, no. 1, pp. 506–516, Feb. 2019, ISSN: 2327-4662, 2372-2541. DOI: 10.1109/jiot.2018.2869003. [Online]. Available: <https://doi.org/10.1109/jiot.2018.2869003>.
- [6] A. Fengler, S. Haghighatshoar, P. Jung, and G. Caire, "Grant-free massive random access with a massive MIMO receiver," in *2019 53rd Asilomar Conference on Signals, Systems, and Computers*, IEEE, Nov. 2019, pp. 23–30. DOI: 10.1109/IEEECONF44664.2019.9049039. [Online]. Available: <https://doi.org/10.1109/IEEECONF44664.2019.9049039>.
- [7] Q. Zhang, S. Jin, and H. Zhu, "A hybrid-grant random access scheme in massive MIMO systems for IoT," *IEEE Open Access*, vol. 8, pp. 88 487–88 497, 2020, ISSN: 2169-3536. DOI: 10.1109/access.2020.2993597. [Online]. Available: <https://doi.org/10.1109/access.2020.2993597>.
- [8] A. Fengler, S. Haghighatshoar, P. Jung, and G. Caire, "Non-Bayesian activity detection, large-scale fading coefficient estimation, and unsourced random access with a massive MIMO receiver," *IEEE Trans. Inf. Theory*, vol. 67, no. 5, pp. 2925–2951, May 2021, ISSN: 0018-9448, 1557-9654. DOI: 10.1109/tit.2021.3065291. [Online]. Available: <https://doi.org/10.1109/tit.2021.3065291>.
- [9] U. K. Ganesan, E. Bjornson, and E. G. Larsson, "An algorithm for grant-free random access in cell-free massive MIMO," in *2020 IEEE 21st International Workshop on Signal Processing Advances in Wireless Communications (SPAWC)*, IEEE, May 2020, pp. 1–5. DOI: 10.1109/spawc48557.2020.9154288. [Online]. Available: <https://doi.org/10.1109/spawc48557.2020.9154288>.
- [10] —, "Clustering-based activity detection algorithms for grant-free random access in cell-free massive MIMO," *IEEE Trans. Commun.*, vol. 69, no. 11, pp. 7520–7530, Nov. 2021, ISSN: 0090-6778, 1558-0857. DOI: 10.1109/tcomm.2021.3102635. [Online]. Available: <https://doi.org/10.1109/tcomm.2021.3102635>.
- [11] G. Callebaut, L. Van der Perre, and F. Rottenberg, "Grant-Free Random Access in Massive MIMO for Static Low-Power IoT Nodes," pp. 46–51, 2021. [Online]. Available: <arXiv%20preprint%20arXiv:2110.07927>.
- [12] E. Björnson, J. Hoydis, and L. Sanguinetti, "Massive mimo networks: Spectral, energy, and hardware efficiency," *Foundations and Trends® in Signal Processing*, vol. 11, no. 3-4, pp. 154–655, 2017, ISSN: 1932-8346. DOI: 10.1561/20000000093. [Online]. Available: <http://dx.doi.org/10.1561/20000000093>.
- [13] T. L. Marzetta, E. G. Larsson, H. Yang, and H. Q. Ngo, *Fundamentals of Massive MIMO*. Cambridge University Press, 2016.
- [14] J. Sherman and W. J. Morrison, "Adjustment of an inverse matrix corresponding to a change in one element of a given matrix," *The Annals of Mathematical Statistics*, vol. 21, no. 1, pp. 124–127, 1950.
- [15] S. Nandi and D. Kundu, *Statistical Signal Processing, Frequency Estimation*. Springer Singapore, 2020, ISBN: 9789811562792, 9789811562808. DOI: 10.1007/978-981-15-6280-8. [Online]. Available: <https://doi.org/10.1007/978-981-15-6280-8>.